Research Article ISSN 2639-9466

Nanotechnology & Applications

Nanomaterials and Rare Earths Used To Evaluate the Photocatalytic Degradation of a Dye, with Potential Use in Decontaminating Water Bodies

Naranjo-Castañeda Felix Antonio[1], Palacios-Grijalva Laura Nadxieli[1], Martínez-Jiménez Anatolio[2*] and Chávez-Sandoval Blanca Estela[3*]

[1]*ITTLA, Ciencias Básicas.*

[2]*UAM, Ciencias Básicas.*

[3]*UAM, Matemáticas Aplicadas y Sistemas.*

***Correspondence:**
Chávez-Sandoval Blanca Estela, Profesora-Investigadora, Titular C, División de Ciencias Naturales e Ingeniería, Depto. Matemáticas Aplicadas y Sistemas, UAM-Cuajimalapa, +5215548101589, E-mail: blanchavez29@gmail.com.

Martínez-Jimenez Anatolio, UAM, Ciencias Básicas, E-mail: amartinez@correo.azc.uam.mx.

Received: 02 February 2021; **Accepted:** 28 February 2021

Citation: Naranjo-Castañeda FA, Grijalva-Palacios LN, Martínez-Jiménez A, et al. Nanomaterials and Rare Earths Used To Evaluate the Photocatalytic Degradation of a Dye, with Potential Use in Decontaminating Water Bodies. Nano Tech Appl. 2021; 4(1): 1-6.

ABSTRACT

In this work, nanomaterials and rare earths were obtained with application in the degradation of dyes since in the developing countries the decontamination of water bodies is essential. We used TiO_2 for incorporation of rare earths applied to photocatalytic activity in degradation of methyl blue due to its high chemical stability and corrosion resistance. We obtain nanostructured materials of TiO_2, TiO_2: Ln^{3+} (Ln^{3+} = Sm^{3+}, Gd^{3+} and Yb^{3+}) by sol gel method, for decontamination of dye such as methylene blue in surface water bodies. Through x-ray diffraction, we found that anatase-rutile phase was achieved in TiO_2 and tetragonal anatase phase in TiO_2: Ln^{3+}. Size average in nanometres of 31, 37, 44 y 34 for TiO_2, TiO_2: Sm^{3+}, TiO_2: Gd^{3+} and TiO_2:Yb^{3+} respectively determinate by atomic force microscopy and by UV spectroscopy the energy gap (2.94, 2.87, 2.85 and 2.95) eV respectively. As for the degradation of the methylene blue dye, the best catalyst under UV radiation was TiO_2: Gd^{3+} with 54% degradation compared to TiO_2 that presented 52%, 29% for TiO_2: Sm^{3+} and with 27% to TiO_2: Yb^{3+} determined by fluorimetry. These materials must be applied in industrial post-treatment processes using photo catalysis for the decontamination of bodies of water.

Keywords

Water decontamination, TiO_2 nanoparticles, Sol-gel synthesis method, Photo catalysis, Methylene blue, Rare earths.

Introduction

Water is a fundamental natural resource of life on Earth, but because we do not allow its cycle to be completed and due to environmental contamination, it is a non-renewable resource, and it is depleted day by day. Its care and treatment are essential to take advantage and reuse in a sustainable way. Unfortunately, there is no adequate management to mitigate the systematic problems due to its increasing pollution caused mainly by domestic and industrial use. Therefore, good quality management is necessary and post treatment in advanced water oxidation processes for disposal.

The most promising and researched option in recent years is to use nanomaterials, because nanoparticles can be synthesized in different sizes and shapes [1], depending on what they will be used since there are many fields in which they are the protagonists [2]. Here we used titanium dioxide (TiO_2) as nanostructured material because it could reduce the water pollution degrade dyes by means of photocatalytic activity under UV radiation [3,4]. Currently nanotechnology involved in TiO_2 doped with rare earths, have a potential application in heterogeneous photo catalysis to degrade organic and inorganic compounds present in contaminant solutions by dyes [5]. Three crystalline phases can present TiO_2: anatase, rutile and brookite. The first two polymorphs have a tetragonal structure while the brookita has an orthorhombic structure. Furthermore, the presence of different trivalent lanthanide cations (Ln^{3+}) of Samarium (Sm), Gadolinium (Gd) and Ytterbium (Yb).

They are host elements in the semiconductor material such is titanium dioxide (TiO_2) [6]. In this work the objective were to synthesize catalysts of pure TiO_2 and doped with Sm^{3+}, Gd^{3+} and Yb^{3+} in contaminated solution with methylene blue, using the low temperature sol gel technique, subsequently characterize the controlled materials and evaluate their photocatalytic performance.

Materials and Methods

Reagents

All reagents were acquired in Sigma Aldrich with high degree of purity, the Titanium tetraisopropoxide "TTIP" ($C_{12}H_{28}O_4Ti$), The Samarium III nitrate hexahydrate ($Sm(NO_3)_3 \cdot 6H_2O$), Gadolinium III hexahydrate nitrate ($Gd(NO_3)_3 \cdot 6H_2O$) and Ytterbium III chloride hexahydrate ($YbC_{l3} \cdot 6H_2O$), the Ethanol (C_2H_5OH), the nitric acid (HNO_3) and the hydrochloric acid (HCl).

Synthesis Sol gel

The pure TiO_2 and doped TiO_2:Ln^{3+} (Ln^{3+} = Sm^{3+}, Gd^{3+}, Yb^{3+}) at 1% molar were obtained by the Sol gel technique in a glass recirculation reactor with coolant. The chemical refrigerant reagents were deposited in stages with magnetic stirring at a temperature of 5°C. During the time of preparation of the sun forming a solution based on TTIP/ethanol and starting the hydrolysis with distilled water. HCl and HNO_3 were used to adjust the pH of the solution, subsequently in a glass crystallizer the samples gelled for 12 h at room temperature and another 12 h (drying stage) at 60°C. Once ready, the materials were crush and calcine at 450°C for 2 h at a heating rate of 5°C/min in atmospheric conditions until obtaining 5 g of each nanostructured material.

Photocatalytic degradation of methylene blue

Methylene blue (MB) was utilized as a model pollutant, to evaluate the photocatalytic activity of all samples of TiO_2 under UV light radiation of 4 W (λ= 250 nm), 10 cm away and environmentally conditioned. In a glass reactor was added 0.128 g of photo catalyst to 100 mL of the MB solution with a concentration of 8.72 mg/L (20%) under constant stirring for three h, taking aliquots every 30 min of 4 mL.

Characterization

The characterization of the nanostructured materials obtained (powders), was performed by X-ray diffraction (DRX), on a diffractometer Philips X'Pert, CuKα radiation, (λ = 1.5046 Å) to 40 kV, 25 mA, 10-80° (2θ), to 5º/min and a step size of 0.02 s. Used an atomic force microscope (AFM) with a Bruker digital instrument scanning probe in 5V Tappin mode. Applying a surface scan of materials obtained with a silicon tip with a nominal radius of less than 10 nm and a resonance frequency between 125-185 KHz. Also used a UV-Vis spectroscopy Varian Cary 100 a range between 200-800 nm in Absorbance (Abs) and mode diffuse reflectance F(R), pre-prepared samples, a DRA-CA-30I integrating sphere accessory.

In a solution of methylene blue in water (43.6 mg/L) at a concentration of 100%, a calibration curve was obtained at different concentrations from 10 to 100% and The Photocatalitic activity was evaluated on an Eclipse Varian Cary fluorescence spectrophotometer with a PMT detector to 766 V, λ_{exc} =672 nm and λ_{emi} =678-860 nm.

Results and Discussion

DR-X

The X-ray diffraction (DR-X) patterns of TiO_2 and Ln^{3+} doped, shows in the figure 1.

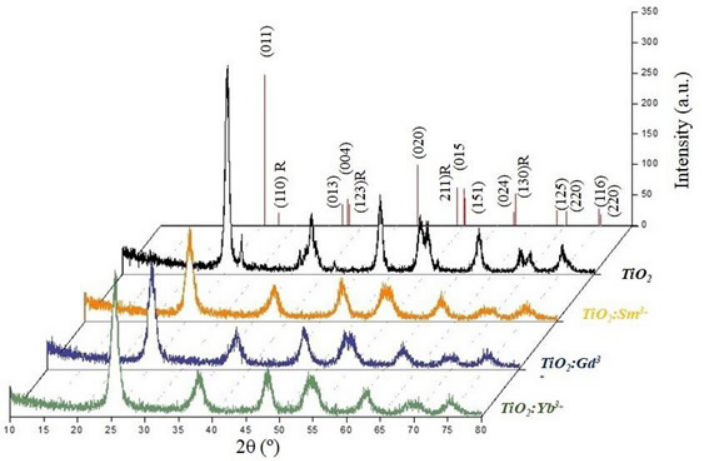

Figure 1: TiO_2 diffraction patterns and TiO_2 doped with Ln^{3+}.

The intensities in the TiO_2 peaks at 2θ are: 25.53°, 27.61°, 36.19°, 38.03º, 41.37°, 48.13º, 54.17°, 55.23°, 56.73º, 62.88°, 68.83°, 70.51º and 75.25º; intensities: 342, 64, 39, 99, 22, 129, 97, 88, 24, 73, 41, 38 y 47; indexed: (011), (110)R, (110), (013)R, (004) R, (020), (211)R, (015), (024), (130)R, (116) and (220) blueprints. It R represents the rutile phase. Confirmed by the Diffraction Data letter of the International Center (ICDD) number 900-8216 anatase fase and 9009-4144 rutile fase. The pure TiO_2 diffractogram clearly shows the intensities of the anatase and rutile phases, both with tetragonal geometry. The other dopant samples with rare earths show a stability of the anatase phase. Mainly in intensity, the highest peak at (0 1 1) corresponding to 2θ: 25. 33º, 25.37º and 25.53º respectively.

The addition of the dopant ions of Ln^{3+} demonstrates that the sol gel technique provides an ideal way to control the structure and stability of the nanostructured material. According to the literature and based on experimental conditions, 1% mol is the optimal concentration that exists and prevents the formation of rare earth oxides on the surface of the TiO_2 semiconductor. Ln^{3+} ions cannot enter the TiO_2 network since the ionic radius of Sm^{3+}, Gd^{3+} and Yb^{3+} (0.964, 0.938 and 0.858) Å respectively. They are larger than Ti^{4+} (0.68 Å). On the other hand, ions can remain on the surface of the crystalline network, as well as on the grain boundary and produce tension in that region, which generally improves the repulsive interaction between doping ions and prevents growth due to the formation of links Ti-O-Sm, Ti-O-Gd and Ti-O-Yb which

in turn results in a decrease in the particle size of nanostructured materials. From the anatase phase, it was determined a = 3.797Å, c = 9.579 Å, ρ = 3.842 g/cm^3, special group I41/amd (141), Z = 4 and V = 136.27 Å3.

AFM

The Atomic Force Microscopy (AFM) images were obtained whit the procedure of the Nano scope v5.33r computer program; a detailed analysis of the section was performed, and the results shows in the figure 2.

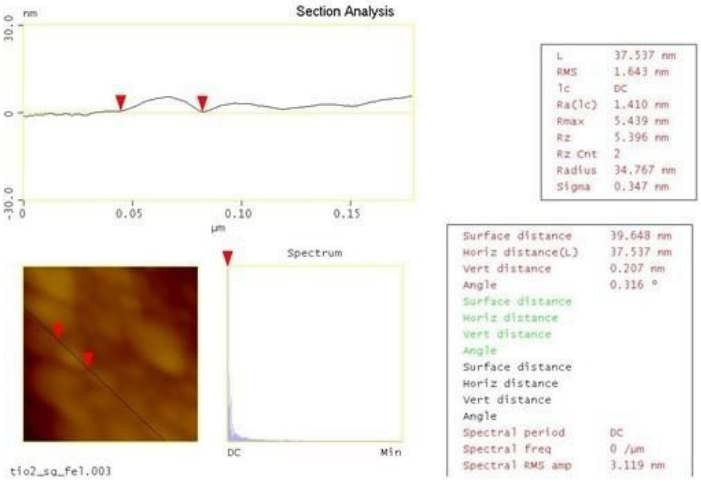

Figure 2: AFM results of measurement of an individual grain.

Figure 3 shows the AFM images in 2D, indicate a good and progressive distribution of the obtained material, the shape of the surface is circular and oval in the nanoparticles of each synthesized sample of the TiO_2 pure and doped with Ln^{3+} (A- D). These images were adjusted in a square area of 0.0625 µm^2 and at a vertical scale of 60 nm.

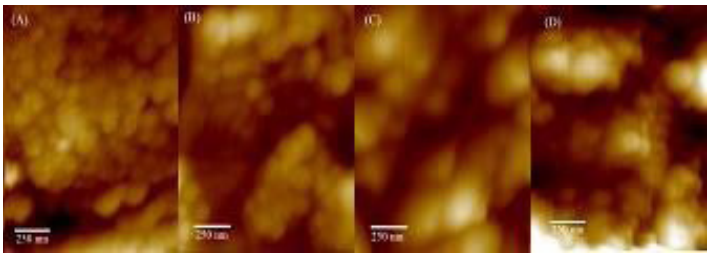

Figure 3: AFM images of catalyst obtained: (A) TiO_2, (B) TiO_2:Sm^{3+}, (C) TiO_2:Gd^{3+} and (D) TiO_2:Yb^{3+}.

The topography of TiO_2 in AFM 3D shows that the surface profile presented a granular distribution and particle agglomerate (Figure 4). Surface morphology and topography are characteristics of the sol gel technique, since the nanoparticles was obtained at low temperature, chemical control and optical properties to the specific photo catalysts [7].

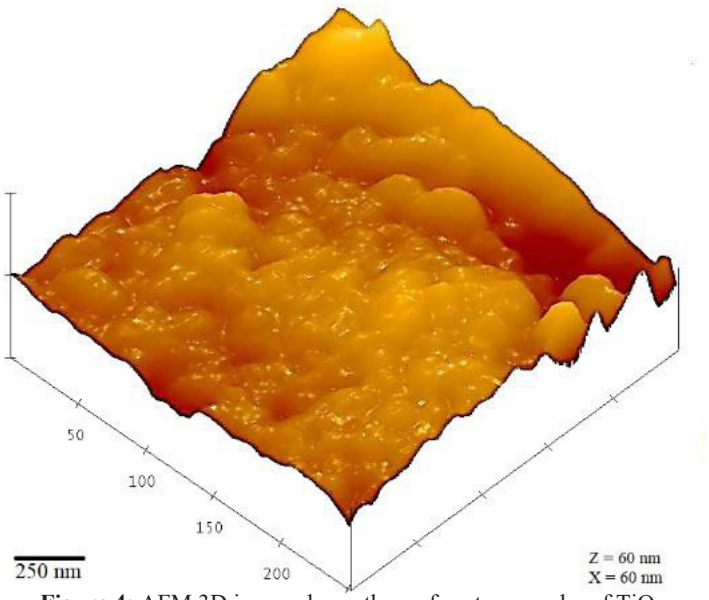

Figure 4: AFM 3D image shows the surface topography of TiO_2.

Each photocatalytic powder material exhibited protruding grains of different diameter sizes (Table 1).

Table 1: Average particle size in each catalyst.

Sample	Size (nm)
TiO_2	31
TiO_2:Sm^{3+}	37
TiO_2:Gd^{3+}	44
TiO_2:Yb^{3+}	34

In addition, ten measurements of the individual particle size were made with which an average was established; there is presence of flat upper flat grains with a dimension slightly less than 37 nm and a height slightly greater than 45 nm, with cavities and roughness being noted. The images showed clear changes in surface morphology based on the addition of the dopant ion Ln^{3+} [7].

UV-Vis

The UV-Vis spectroscopy (Figure 5), allow that whit the wavelength (λ) we calculate and determine the energy gap (Eg). Therefore, it is important to change the conversion of λ (nm) to energy units (eV) to multiplying the value by the constant of the Plan in eV by the constant of the speed of light (nm). Absorption was observed in all materials but was better detailed in the range between 395-455 nm and the TiO_2 has a maximum at 363 nm, region corresponding to near UV. The lanthanide-doped materials exhibited maximum values of 357, 356 and 359 nm. On the other hand, the diffuse reflectance numerical data F(R) was used to make an adjustment according to Kubelka-Munk (F(R)x hv)1/2 vs Eg (eV) then divide it between the range of 600 nm of the UV-Vis test, obtaining the value in eV.

It is considered that synthesized materials may contain indirect transitions with linear adjustments. This is due to the fact that the spectral tendency proposes the activation of the material by light photons that affect the sample at the time of measurement.

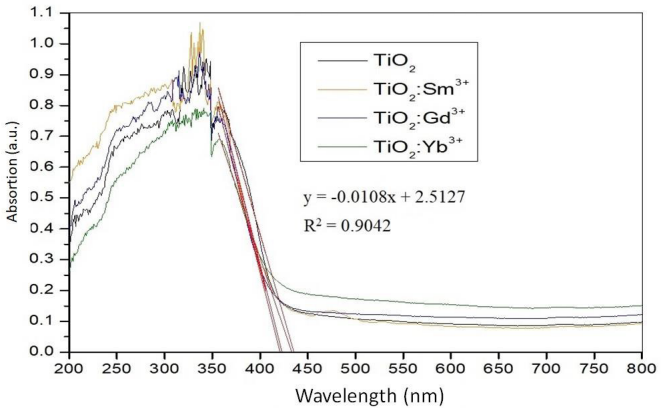

Figure 5: Uv-Vis absorption spectra.

The Eg values of the materials nanostructured are presented in table 2. All of them were adjusted, established by the electron-electron/hole (e-/h+) change behavior that occurs in the nanoscale and the effect action by the doping ion of each lanthanide on TiO_2.

Table 2: Energy gap values of the photo catalysts obtained by UV-Vis absorption spectroscopy and Kubelka-Munk in (eV).

Methode	TiO_2	$TiO_2:Sm^{3+}$	$TiO_2:Gd^{3+}$	$TiO_2:Yb^{3+}$
Abs	2.94	2.87	2.85	2.95
Kubelka-Munk	3.03	3.08	3.11	3.14

The indirect transition to observe the behaviour of each material was considered by [8]. It is reported that TiO_2 contains 3.03 eV, optimal energy for its application in photo catalysis. The indirect effect is evaluated in the Eg value for photocatalytic capacity, following the mechanism of electronic excitation in the conduction band with direction to the valence band.

In the figure, 6 it is noted the function of Kubelka-Munk considering the indirect interactions in the diffuse reflectance, making the linear adjustment corresponding to the samples at 421, 422, 432 and 435 nm. In comparison with the Eg values of when the Sol-gel synthesis there is variation in the precursor, in the acid concentration and in the concentration of doping ion close to 1%. A value of 3.02 Eg was determined in the crystalline phases of anatase-rutile.

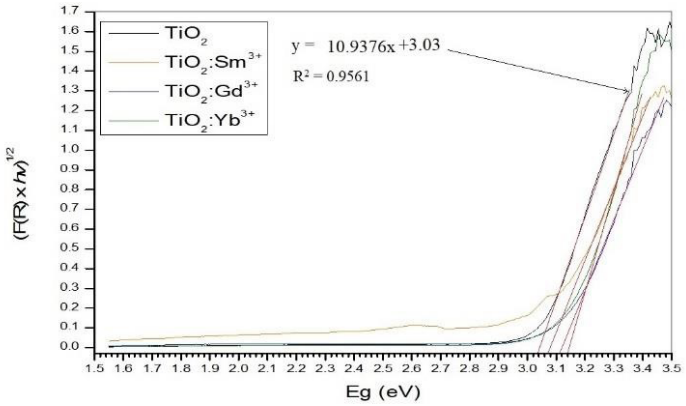

Figure 6: Graphical representation of Kubelka-Munk (F(R) x hv) 1/2 vs Eg (eV).

Fluorescence spectroscopy

Nanostructured samples obtained, also was characterized by fluorescence spectroscopy (Figure 7) in a range between 400-600 nm, slit = 2.5 and λexc = 380 nm. Different intensities were identified at 405, 421, 485 and 518 nm (17.84, 18.45, 14.97 and 18.61) in TiO_2, $TiO_2:Sm^{3+}$, $TiO_2:Gd^{3+}$, $TiO_2:Yb^{3+}$ respectively. However, the lower emission intensity represents the blue line doped with Gd^{3+}. They represent energy transitions, which can start in the conduction band directed towards the valencia band, by means of different photons that emit hv energy characteristic of each material [9].

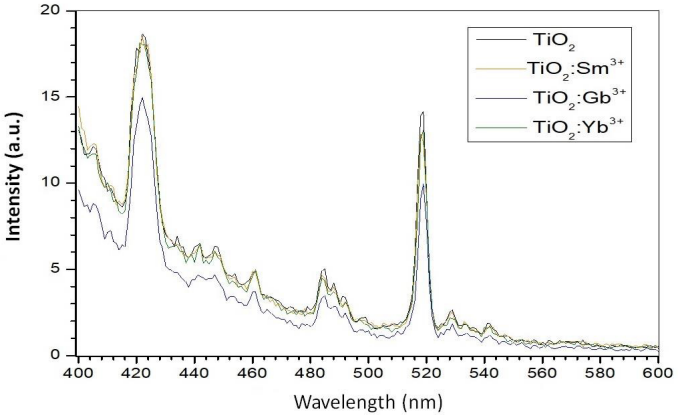

Figure 7: Fluorescence spectra of the catalysts obtained.

Photocatalytic evaluation

The testing carried out using the heterogeneous method of photo catalysis involved in the degradation of methylene blue dye ($C_{16}H_{18}ClN_3S{\cdot}3H_2O$) with a molecular weight of 373.91g/mol, under UV radiation, shown degradation in the molecule, like reported by Wang et al. 2018.

In the figure 8 shows the Calibration curve.

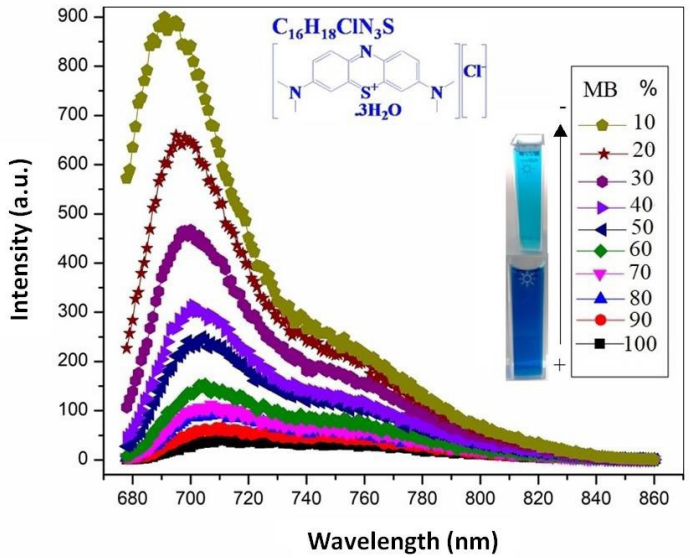

Figure 8: Emission spectrum: calibration curve with respect to the MB concentration.

Figure 9 shows the asymmetric trend between intensity and wavelength with respect to each MB concentration, made from the analysis and based on the considerations of other authors [10].

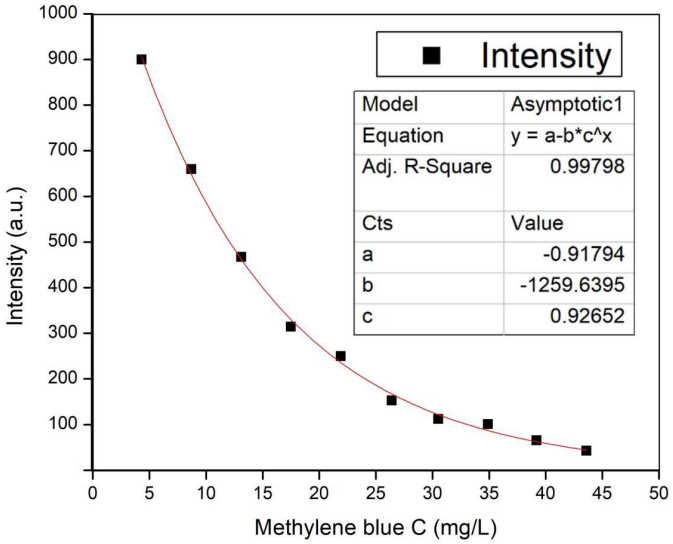

Figure 9: Emission Intensity vs MB concentration.

The concentration of 20% (8.72 mg/L) was the best to colour degradation. The maximum absorption length corresponded to 664 nm and the maximum peak at 668 nm recorded by fluorescence emission. A maximum excitement to 680 nm and a maximum emission of 789 nm indicates that the catalyst has a decrease in emission intensity [11].

The results by fluorescence spectroscopy in emission of pure TiO_2 and doped with Ln3+ were absorbed with respect to each dopant ion, but each one presented its own luminescence properties in relation to the electronic transitions that allowed a photocatalytic activity effective, according to reported by [12].

Definitely, the contribution of UV radiating light is an important factor for photocalitic activity, because it is a source of energy that causes activation by valence electrons and tends to be excited to perform a simultaneous decomposition in an oxide reduction process applied to the reduction mechanism MB reaction by the catalysts mentioned.

To improve the fluorescence of the activated ions, the concentration of the ions in the polymer matrix should be increased; the fluorescence intensities also adhere to a higher concentration of the sensitizer. However, the ion concentration does not affect the cooling center, but sensitizing (secondary) ions must be controlled as aggregation centers as recommended by Marcelino and Amorim 2019 [13].

Figure 10 shows the emission fluorescence spectroscopy and the best performing material was TiO_2:Gd^{3+}. In addition, different intensities were observed with respect to wavelength at different degradation times. There is a decrease in concentration. Notice that the black line at time zero is the most intense, indicates the concentration of 20% of the dye. The decreases of the curves in the intensities that depend on the degradation time for 3 hours was also detailed.

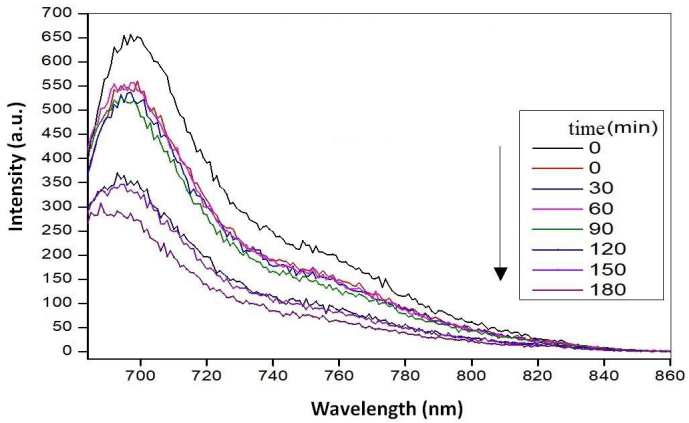

Figure 10: TiO_2:Gd^{3+}/MB emission fluorescence spectroscopy.

Kinetics of degradation (C/C0) of the dye MB

Figure 11 shows the degradation behavior during 3 h of the photocatalysts with respect to the initial concentration of the MB dye. A decrease in concentration is observed in the first 30 min, later, it stabilized to a behavior with a tendency to decrease linearly, mainly due to TiO_2. On the other hand, look at the kinetics of TiO_2: Gd^{3+}. It was the most appropriate. Ben et al., [10], reported that Gd- TiO_2 imposed a 5% better yield of photocatalytic activity with an 80% reduction in MB concentration after 6 h irradiation.

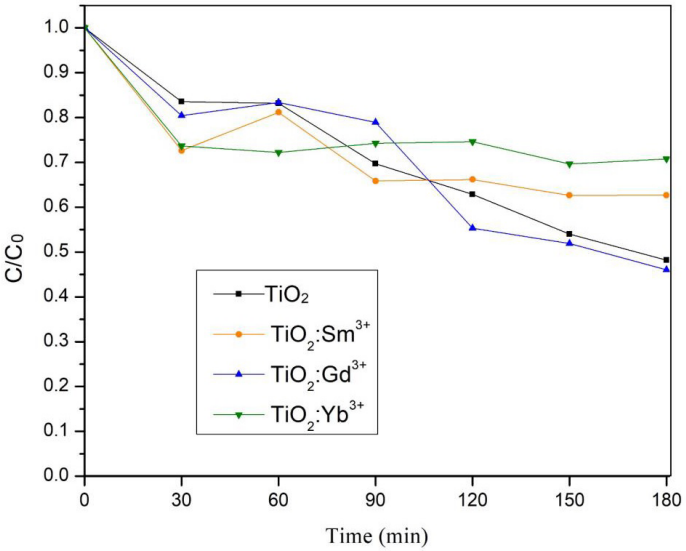

Figure 11: Degradation of MB by pure TiO_2 and doped with Ln^{3+}. 241.

Photocatalytic degradation of the MB dye by TiO_2 materials involves the process of forming free electron pairs on the surface of each of the materials, promoting the attack of hydroxyl and superoxide radicals that lead to dye degradation. Furthermore,

the mechanism of the Ln^{3+} ions could improve the photocatalytic activity until obtaining compounds of CO_2, H_2O, SO_{2-} and NO_{3-} as reported by Kaur et al., 2018 [14].

Conclusions

Pure TiO_2 and doped TiO_2:Ln^{3+} (Ln^{3+}= Sm^{3+}, Gd^{3+} e Yb^{3+}) particles were synthesized by the sol gel method. The main conclusions in this research work are: DR-X determined the combination of the anatase and rutile phase in pure TiO_2, but by adding the Ln^{3+} ions. I stabilize the anatase phase with tetragonal symmetry. AFM showed a good distribution of particles, morphology and different sizes of synthesized materials. The energy gap values (Eg) were determined by UV-Vis and the method of Kubelka-Munk very close to what was reported in relation to TiO_2 materials. Fluorescence emission analysis reveals the characteristic intensities and lengths of each pure and doped material with Ln^{3+} in powder form and when present under photocatalytic activity by degradation of the MB dye. The photocatalytic process depends largely on the size of the dopant ion; the hydroxyl groups present on the surface attack the contaminant. Finally, the best-synthesized material involved in the photocatalytic application that revealed the best results was TiO_2:Gd^{3+} with 54% degradation compared to TiO_2 that presented 52%, 29% for TiO_2:Sm^{3+} and with 27% corresponding to TiO_2:Yb^{3+}.

Perspectives

As know the factors that could improve the photocatalytic activity of nanostructured materials are principally calcination, concentration, pH, precursor, nature of the solvent and UV radiation, and the Eg interval, of cationic doping is responsible for the displacement of the conduction band.

Therefore, it is necessary to improve the excitation of materials by light in the UV region and near the visible one; avoiding recombination (e-/h+), sensitizing the photo reduction-oxidation processes, since the materials have some defects and oxygen vacancies, this will create characteristic vacuum states that will allow the simultaneous jump of energy from each material.

Data Availability Statement (DAS)

The data that support the findings of this study are available on request from the corresponding author, BECS. The data are not publicly available due to containing information that could compromise the privacy of research participants.

Acknowledgements

To CONACYT for the grant 706588 to Naranjo-Castañeda F.A. In the master's program in Engineering Sciences.

References

1. Chávez-Sandoval BE, Ibáñez-Hernández MMA, García-Franco F, et al. Biological Synthesis and Characterization of Gold Nanoparticles (AuNPs), Using Plant Extracts. Journal of Nanomaterials & Molecular Nanotechnology. 2016; 5:
2. Chávez-Sandoval BE, Balderas-López JA, García-Franco F, et al. The pH role about synthesis, distribution, and potential applications of gold nanoparticles. Int. J. Biomedical Nanoscience and Nanotechnology (IJBNN). 2020; 4: 120-137.
3. Ameta R, Ameta SC, "Photocatalysis. Principles and applications." CRC Press. Taylor & Francis Group. 2017; 1-96.
4. Ahmada W, Kumar J K, Soni S, "Green synthesis of titanium dioxide (TiO_2) nanoparticles by using Mentha arvensis leaves extract and its antimicrobial properties." Inorg Nano-Tec Che. 2020; 50: 1032-1038.
5. Domínguez F R, Palacios-Grijalva L N, Martínez J A. "Photocatalytic degradation of Rhodamine B under UV irradiation over anatase TiO_2:Ln3+ nanoparticles." J of Ph C Series. 2019; 1221: 012021.
6. Bergman L, McHale J L. Handbook of Luminescent Semiconductor Materials. "Photoluminescence and Carrier Transport in Nano crystalline TiO_2." CRC Press. 2011; 13: 365-385.
7. Cano-Casanova L, Amorós-Pérez A, Lillo-Ródenas M, et al. "Effect of the Preparation Method (Sol-Gel or Hydrothermal) and Conditions 307 on the TiO_2 Properties and Activity for Propene Oxidation". Materials. 2018; 11: 2227.
8. Aristanti Y, Supriyatna Y I, Masduki N P, et al. Effect of calcination temperature on the characteristics of TiO_2 synthesized from ilmenite and its applications for photocatalysis. IOP C Series: Mater Sci. Eng. 2019; 478: 012019.
9. Araújo D dos S, Diniz V C de S, Torquato R A, et al. "Avaliação gap óptico do TiO_2 obtido pelo método Pechini: influência da variação das fases anatásio-rutilo." Matéria. 2018; 23: e-11949.
10. Ben C M, Messaoud M, Wethimuni M L, et al. "Preparation and characterization of photocatalytic Gd-doped TiO_2 nanoparticles for water treatment." Environ Sci Pollut R. 2019; 26: 32734-32745.
11. Bi Y, Westerhoff P. "Hight-throughput analysis of photocatalyticreactivy of difrfrering TiO_2 formulation using 96-well microplate reactors." Chemosphere. 2019; 223: 275-284.
12. Ammari Y, El Atmani K, Bay L, et al. "Elimination of a mixture of two dyes by photocatalytic degradation based on TiO_2 P- 25 Degussa." Mater Today: Proceedings. 2019; 22: 126-129.
13. Marcelino, R. B. P., and Amorim, C. C. Towards visible-light photocatalysis for environmental applications: band-gap engineering versus photons absorption—a review, Environ Sci Pollut Res. 2019; 26: 4155-4170.
14. Kaur H, Kumar S, Verma N.M, et al. Role of pH on the photocatalytic activity of TiO_2 tailored by W/T mole ratio, Journal of Materials Science: Materials in Electronics 29, 16120-16135.